Erratum

Reversed functional topology in the antennal lobe of the male European corn borer

Z. Kárpáti, T. Dekker and B. S. Hansson

10.1242/jeb.025049

There was an error published in *J. Exp. Biol.* **211**, 2841-2848.

The accepted date should have read 4 July 2008 not 4 July 2007.

We apologise to the authors for this error.

The Journal of Experimental Biology 211, 2841-2848
Published by The Company of Biologists 2008
doi:10.1242/jeb.017319

Reversed functional topology in the antennal lobe of the male European corn borer

Zsolt Kárpáti[1,2,*], Teun Dekker[1,*,†] and Bill S. Hansson[1,3]

[1]Division of Chemical Ecology, Swedish University of Agricultural Sciences, PO Box 44, SE-230 53, Sweden, [2]Plant Protection Institute of Hungarian Academy of Sciences, PO Box 102, H-1525, Budapest, Hungary and [3]Max Planck Institute for Chemical Ecology, Department of Evolutionary Neuroethology, Hans-Knoell-Strasse 8, D-07745 Jena, Germany

*These authors contributed equally to this work
†Author for correspondence (e-mail: teun.dekker@ltj.slu.se)

Accepted 4 July 2007

SUMMARY

The European corn borer *Ostrinia nubilalis* (Hübner) is a model of evolution of sexual communication in insects. Two pheromone strains produce and respond to opposite ratios of the two pheromone components, Z11 and E11-tetradecenylacetate. The Z-strain uses a ratio of 97:3 of Z11:E11 tetradecenylacetate, whereas the E-strain uses a ratio of 1:99. We studied how the difference in male preference correlates with differences in wiring of olfactory input and output neurons in the antennal lobe (AL). Activity-dependent anterograde staining, intracellular recording and immunocytochemistry were used to establish the structure and function of male olfactory receptor neurons (ORNs) and AL projection neurons (PNs). Physiologically characterized neurons were reconstructed using confocal microscopy of α-synapsin stained ALs. The ALs of males and females in both strains had approximately 64 glomeruli. In males the macroglomerular complex (MGC) was morphologically similar in the two strains and consisted of two major compartments, a large, medial compartment folded around a smaller, lateral one. Extensive physiological and morphological analysis revealed that in both strains the major pheromone component-specific ORNs and PNs arborize in the medial MGC glomerulus, whereas those sensitive to the minor pheromone component arborize in the lateral glomerulus. In other words, the two strains have an indistinguishable MGC morphology, but a reversed topology. Apparently, the single-gene-mediated shift that causes a radical change in behavior is located upstream of the antennal lobes, i.e. at the ORN level.

Key words: olfaction, antennal lobe, electrophysiology, neuroanatomy, *Ostrinia nubilalis*, polymorphism, olfactory receptor neuron, projection neuron, intracellular recording, evolution.

INTRODUCTION

Moth pheromone communication is a schoolbook example of sexual selection and speciation. Many salient examples illustrate how evolutionary forces mold the female pheromone production as well as the male response to inter- and intraspecific signals. In addition, the moth pheromone system offers unique possibilities for studying the evolution of olfactory processing and its behavioral correlate, as the organization of the corresponding olfactory subcircuitry is relatively simple and behavioral responses to pheromones generally robust. Yet, the proximate mechanisms underlying shifts in pheromone preference are still elusive.

Sex pheromone components are detected by olfactory receptor neurons (ORNs), which, like other ORNs in insects, project into the first olfactory neuropil, the antennal lobe (AL), through the antennal nerve (AN) (Bretschneider, 1924). The AL comprises a number of glomeruli in which synaptic contacts between ORNs, projection neurons (PNs) and local interneurons are made. Male moths have a few enlarged glomeruli, which make up the macroglomerular complex (MGC), situated at the entrance of the AN. These glomeruli are dedicated to receiving information regarding female-produced sex pheromones (Bretschneider, 1924; Koontz and Schneider, 1987). In several moth species, the number of MGC glomeruli equals the number of behaviorally relevant pheromone components, with each ORN type projecting to one MGC glomerulus (Hansson et al., 1992; Ochieng et al., 1995; Todd et al., 1995; Berg et al., 1998). The ORNs project into the AL, where input is relayed onto PNs. Blend-specific PNs, which may be involved in blend recognition, have been found in several noctuid species (Christensen et al., 1989; Christensen et al., 1991; Hansson et al., 1994b; Anton and Hansson, 1994; Anton and Hansson, 1995; Wu et al., 1996).

The European corn borer, *Ostrinia nubilalis* Hübner (Lepidoptera: Pyralidae) has two sex pheromone components (*Z*)-11- and (*E*)-11-tetradecenyl acetate (Z11- and E11-14:OAc) and an interspecific behavioral antagonist (*Z*)-9-tetradecenyl acetate (Z9-14:OAc) (Glover et al., 1989). The species occurs in two strains that use opposite pheromone component ratios. Females of the Z-strain produce 97% Z11-14:OAc and 3% E11-14:OAc whereas E-strain females produce 99% E11-14:OAc and 1% Z11-14:OAc (Anglade et al., 1984; Klun and Robinson, 1971; Klun et al., 1973). Consequently, the strains do not freely interbreed in sympatry (Cardé et al., 1978; Malausa et al., 2005).

Males of both strains have three types of sensilla trichodea on their antenna (type C, B and A) which each contain one, two or three neurons, respectively, responding to pheromone stimuli (Hansson et al., 1987; Hansson et al., 1994b). Sensillum type A contains three ORNs, the neuron characterized by a large spike amplitude responds to the major component, the neuron having a intermediate spike amplitude responds to the minor pheromone component; the third ORN produces small amplitude spikes in response to the behavioral antagonist. Sensillum type B houses two ORNs, one large spiking ORN responding to the major component, and a small-spiking ORN responding to the minor pheromone component. Sensillum type C contains one ORN responding either to the major pheromone component or to the behavioral antagonist (Hansson et al., 1987; Hallberg et al., 1994; Cossé et al., 1995).

Genetic studies of the *O. nubilalis* pheromone communication system have indicated that female sex pheromone production and the male sensory setup are primarily controlled by a single autosomal factor (Hansson et al., 1987; Roelofs et al., 1987; Löfstedt et al., 1989; Roelofs and Glover, 1991).

Previous studies described the AL of *O. nubilalis* (Anton et al., 1997). However, the techniques at that time did not allow a clear resolution of the intricate structure of the MGC in this species. Here, we resolve in much more detail the neuroanatomy of the AL of the male and female European corn borer. Also, we morphologically and physiologically characterize pheromone sensitive ORNs and PNs. The results demonstrate that the single-gene-mediated shift is located upstream of the antennal lobes, i.e. at the level of the ORN.

MATERIALS AND METHODS

Insects

The Z- and E-strains of European corn borer, *Ostrinia nubilalis* Hübner (Lepidoptera: Pyralidae) were reared in the laboratory. The Z-strain culture originated from a 2004 adult collection from corn fields in Kéty, Tolna, Hungary. The E-strain was kindly provided by Dr Wendell Roelofs and originated from a collection of larvae, pupae and adults from corn stubble in New York state, USA. The cultures were maintained on a semi-artificial diet (Mani et al., 1978) at 25°C, RH 70% under a 18 h:6 h L:D photoperiod. The genetic purity of the cultures was monitored by gas chromatographic analysis (GC) of pheromone production in females.

Sexes were separated as pupae and kept in separate plastic boxes to avoid exposing adult males to female sex pheromone. Adults were fed 5% honey water solution throughout their adult lives. Moths of 1–4 days old were used.

Activity-dependent anterograde stainings of olfactory receptor neurons

Previous studies using antennal staining have demonstrated that under pulsed odor stimulation there is a preferential staining of the neuron sensitive to the stimulus (Hansson et al., 1992; Hansson, 1997; Kirschner et al., 2006). Two techniques were used to obtain activity-dependent stains. A single sensillum from the second or third flagellar segment was characterized physiologically, after which a glass electrode stained with 1% neurobiotin (Molecular Probes, Carlsbad, CA, USA) in 0.25% KCl was placed over the sensillum. Alternatively, a small neurobiotin crystal was placed on the second or third flagellar segment between pheromone-sensitive sensilla. The animal was kept for 1 h under continuous pulsed (0.2 s stimulus, 4 s clean air, total flow 8 ml s^{-1}) stimulation with 100 ng of either Z11- or E11-14Ac. Moist filter paper surrounded the preparation to avoid dehydration and crystallization. Subsequently, the moths were decapitated and the heads were processed as described under 'neuroanatomical techniques'. The success rate of specific stainings of single ORNs was low (~14%). However, in preparations with multiple ORN stains, in every case where the axonal projections could be traced each ORN was found to arborize uniglomerularly.

Intracellular recording

A male moth was restrained in a plastic pipette tip. The moth was inserted from the wide end of the pipette tip with the head protruding from the tip. The head was immobilized with dental wax (Surgident, Heraeus Kulzer, Inc., Armonk, NY, USA). The proboscis and one of the antennae were cut off and the scales on the head were removed. Incisions between the eyes were made creating a window through which the antennal lobes were visible. The muscles around the antenna were removed to allow for stable recordings. The moth was placed in an electrophysiological setup and the opened head was superfused with a ringer solution of pH 6.9 containing 8.55 g l^{-1} sucrose (Christensen and Hildebrand, 1987). The odorants were diluted in redistilled n-hexane and applied on a filter paper disc inside a Pasteur pipette. A 0.5 s stimulation was delivered at 4 ml s^{-1} into a charcoal-filtered humidified air stream (0.5 ml min^{-1}) flowing over the ipsilateral antenna of the moth through an opening 20 cm from the antenna. The odor stimuli were presented at 10 s inter-stimulus intervals. Stimuli included Z11-14:OAc, E11-14:OAc and blends thereof, and Z9-14:OAc at a range of concentrations (1 ng–10 μg). A hexane blank served as control. The purity of the odorants was verified using GC. The recordings followed the procedures described by Christensen and Hildebrand (Christensen and Hildebrand, 1987). Glass electrodes were stained with 1 mol l^{-1} KCl, with the tip containing 1% neurobiotin. Using a micromanipulator, the recording electrode was inserted into the antennal lobe close to the point of entry of the antennal nerve, where many PN dendrites coalesce from the MGC. Usually, the most successful recordings were obtained with the electrode situated close to the surface. When intracellular contact was established, the ipsilateral antenna was stimulated and the activity of the neuron before, during and after stimulation was observed. The signal was amplified, digitally converted (IDAC-4 USB, Syntech, Kirchzarten, Germany) and visualized using a PC with AutoSpike 3.2 software (Syntech). Recordings of action potentials were stored on the PC and analyses were performed using AutoSpike software. The spikes were counted manually. The response of PNs was expressed as the number of spikes during an 0.25 s period after stimulus onset minus the number of spikes 0.25 s before stimulus onset (which represents the spontaneous activity of the neuron) and expressed as the number of spikes per second. Physiologically characterized neurons were stained with neurobiotin by passing 0.5–1.2 nA of constant depolarizing current through the recording electrode for 10–15 min. Brains were processed as described under 'neuroanatomical techniques'.

Neuroanatomical techniques

Heads of decapitated moths were fixed in 4% formaldehyde containing 0.25% Triton X-100 in PBS overnight at 4°C and then dissected, washed 4×10 min in 0.25% Triton X-100 in PBS and incubated in PBS (0.25% Triton X-100) with 5% α-synapsin (courtesy of Dr Buchner, University of Würzburg, Germany) antibody and 3% fluorescein Avidin (Invitrogen, Carlsbad, CA, USA) overnight on a rotator at room temperature. The next day, brains were washed 4×10 min in PBS (0.25% Triton X-100); incubated with 1% α-mouse (goat) Alexa Fluor 546 (Invitrogen) in PBS (0.25% Triton X-100) for 4 days at 4°C. Finally the brains were washed 4×10 min in PBS (0.25% Triton X-100) and mounted in Vectashield Hard set (Vector Laboratories, Burlingame, CA, USA).

The mounted brains were examined under a Zeiss LSM 510 confocal microscope (Carl Zeiss, Jena, Germany) equipped with a 40×, 1.4 oil-immersion DIC objective lens. Structures indirectly labeled with fluorescein Avidin and Alexa Fluor 546 and were excited with an argon (488 nm) and a helium–neon laser (543 nm) and their fluorescence was detected after passing through a band pass (505–530 nm) and a long pass (560 nm) filter, respectively. Stacks of 50–200 confocal images were scanned and the images were stored at a size of 1024×1024 pixels. The three-dimensional reconstructions were done with AMIRA (Mercury Computer Systems SAS, Merignac Cedex, France) with 512×512 pixels image stacks. Every second section was reconstructed.

In each optical section, contours of glomeruli were demarcated by hand (i.e. image segmentation). The volumetric measurements were done using AMIRA software.

RESULTS

The antennal lobe of Z-strain *O. nubilalis*

First, we elucidated the architecture of the primary olfactory neuropil, the antennal lobe (AL). α-Synapsin antibody staining penetrated the tissue well and enabled visualization of the entire *O. nubilalis* AL (Fig. 1A). Deeper, more posterior in the AL, where α-synapsin penetration and staining was weaker, phalloidin staining was helpful in resolving the glomerular boundaries. Based on our AMIRA reconstructions we estimated the number of glomeruli in Z-strain female and male *O. nubilalis* AL to be ~64 and ~66, respectively (Fig. 1). It should be noted that the precise number of identified glomeruli differed somewhat between preparations as a result of differences in the quality of staining, especially of more posterior glomeruli.

At the point where the AN enters the AL, Z-strain male *O. nubilalis* have a much larger set of glomeruli, the MGC known to be exclusively involved in sex pheromone processing. Three MGC glomeruli could be distinguished. Two large, highly convoluted and interdigitated glomeruli, variable in shape and dimension ($297\times10^3\pm36\times10^3\,\mu m^3$, $141\times10^3\pm17\times10^3\,\mu m^3$, N=3; Fig. 1B), one medial and one lateral. The accuracy of the demarcations of these two large glomeruli was corroborated using the stains of specific PNs (see below). A third large disc-shaped glomerulus was located posterior of the two large interdigitated glomeruli ($89\times10^3\pm3.4\times10^3\,\mu m^3$, N=6; Fig. 1C). Inexplicably, the medial glomerulus was always more strongly stained with α-synapsin than the lateral glomerulus (Fig. 1A,D). In females, two enlarged female glomeruli (LFGs) were found at the entrance of the AL. LFG1 had

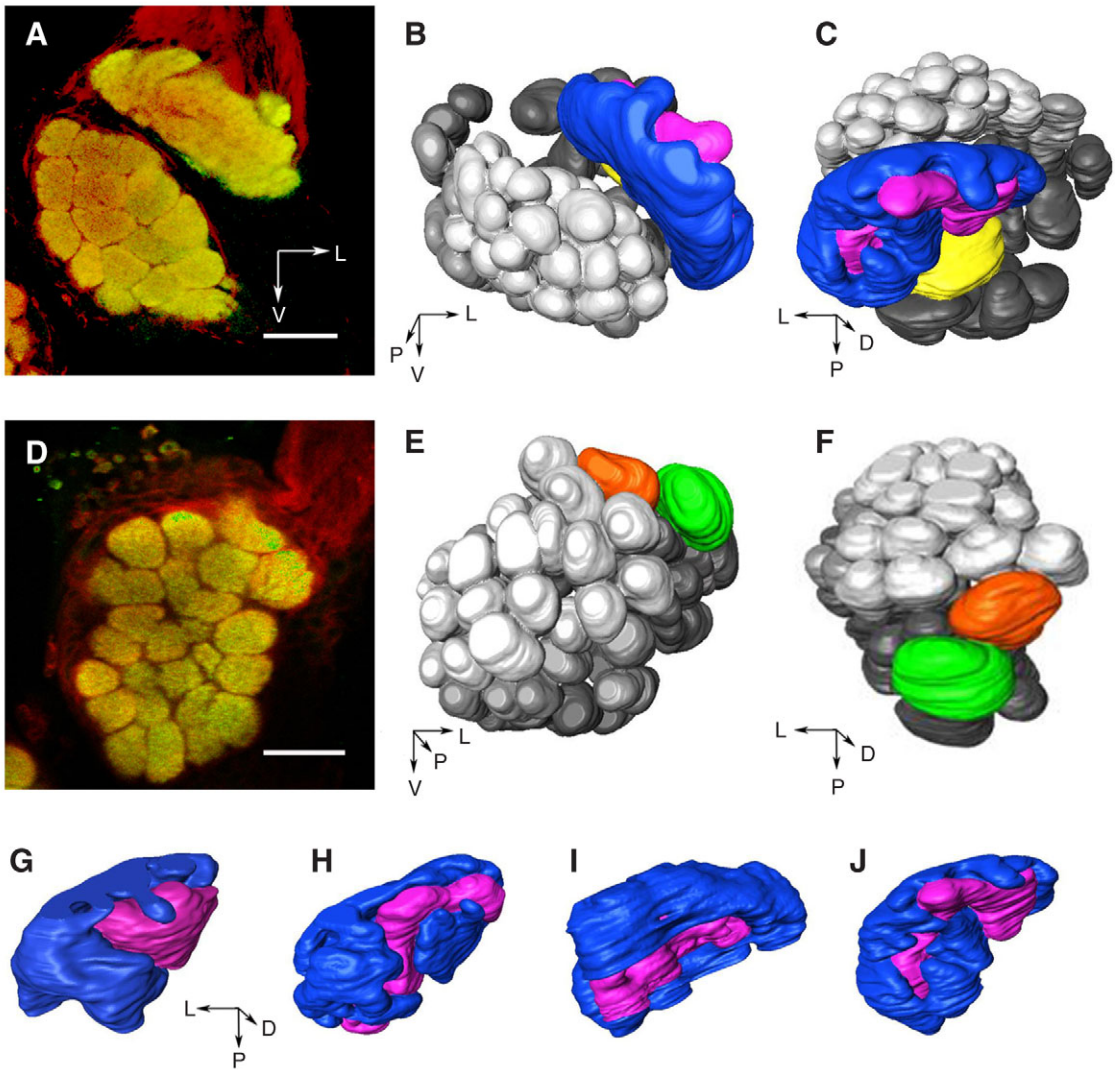

Fig. 1. The antennal lobe (AL) of male and female Z-strain *O. nubilalis*. (A) Confocal section through a male AL. Overview staining: in green α-synapsin labeled with Alexa Fluor 488, and in red phalloidin conjugated to Alexa Fluor 546. (B,C) Three-dimensional reconstruction of the male AL in A. In pink and blue are the two large intertwined macroglomerular complex (MGC) glomeruli; in yellow, the smaller posterior MGC glomerulus. Ordinary glomeruli are depicted in gray, with darker shading indicating more posterior positions. Orientation: L, lateral; V, ventral; D, dorsal; P, posterior. (D) A confocal section through a female AL. Overview staining as in (A). (E,F) Three-dimensional reconstruction of the female AL in D. In green and orange are the two large female glomeruli (LFG1 and 2, respectively). Ordinary glomeruli are depicted in gray, with darker shading indicating more posterior positions. (G–J) Three-dimensional reconstructions of the MGC of four different males. Note the variability in structure. Scale bars, 50 μm.

an estimated volume of $64\times10^3\,\mu m^3$, which was on average 4.4 times larger than an ordinary glomerulus (average radius of $15\,\mu m^3$; Fig. 1D). LFG2 had an estimated volume of $53\times10^3\,\mu m^3$ (Fig. 1E,F).

Functional characterization of Z-strain male macroglomerular complex input and output

Activity-dependent anterograde stainings of antennal sensilla using neurobiotin were used to establish the pattern of ORN arborizations in the MGC (Fig. 2A,B; Table 1). ORNs exclusively arborized in either the medial or lateral glomerulus. Single ORNs stained under stimulation with Z11-14:OAc arborized in the medial glomerulus, whereas stimulation with E11-14:OAc resulted in staining of the ORNs arborizing in the lateral glomerulus.

Extensive projection neuron (PN) recordings (538 contacts in total; Fig. 3F, Table 1, Fig. 4) were conducted and physiologically well-characterized PNs were stained with neurobiotin tracer. PN arborizations were checked against a background of α-synapsin staining. The stainings demonstrate that without exception Z11-14:OAc-specific PNs arborize in the medial glomerulus (Fig. 3A), whereas E11-14:OAc-specific PNs arborize in the somewhat smaller lateral glomerulus (Fig. 3B). The soma of specific neurons were located in the medial cell cluster. Specificity was evidenced in at least a 10^1–10^3-fold difference in sensitivity to Z11- and E11-14:OAc. Neurons responding equally to both E11- and Z11-14:OAc were mostly local interneurons arborizing in most, if not all glomeruli. On rare occasions (two intracellular recordings, three successful stains) we encountered PNs that were more sensitive to a blend of Z11- and E11-14:OAc than either of the components separately (Fig. 3E). These PNs arborized in both the lateral and medial MGC glomeruli, sometimes apparently also in an ordinary glomerulus. The cell bodies of these PNs were located in the lateral cell cluster (Fig. 3E). Few recordings were obtained from PNs responding only to the antagonist, Z9-14:Ac. Only two stainings were obtained of an antagonist specific PN, with dendritic arborizations in the posterior disc-shaped glomerulus only (in yellow in Fig. 1C). However, the quality of the staining and dissection did not allow for reconstruction.

The neuroanatomy and physiology of the macroglomerular complex of E-strain *O. nubilalis*

Overview staining with α-synapsin demonstrated that the architecture of the antennal lobes in the E-strain was highly similar to that of the Z-strain. The total volume of the MGC was similar in the two strains (Table 2). Activity-dependent neurobiotin stains of ORNs showed, similar to those from the Z-strain, that ORNs display uniglomerular arborizations, but with E11-14:OAc-sensitive ORNs projecting into the medial glomerulus, and Z11-14:OAc-sensitive neurons to the lateral glomerulus (Fig. 2C,D). The success rate of activity-dependent stains was low. However, the physiological characterization of peripheral input to the AL was totally corroborated by stains of physiologically characterized PNs. We recorded from a total of 1278 PNs. Twenty stainings of PNs responding specifically to one of the two pheromone components yielded a total of five single PN stainings (Table 1, Fig. 4). Specific neurons arborized again exclusively in one MGC glomerulus, with E11-14:OAc-responding PNs sending dendritic branches into the

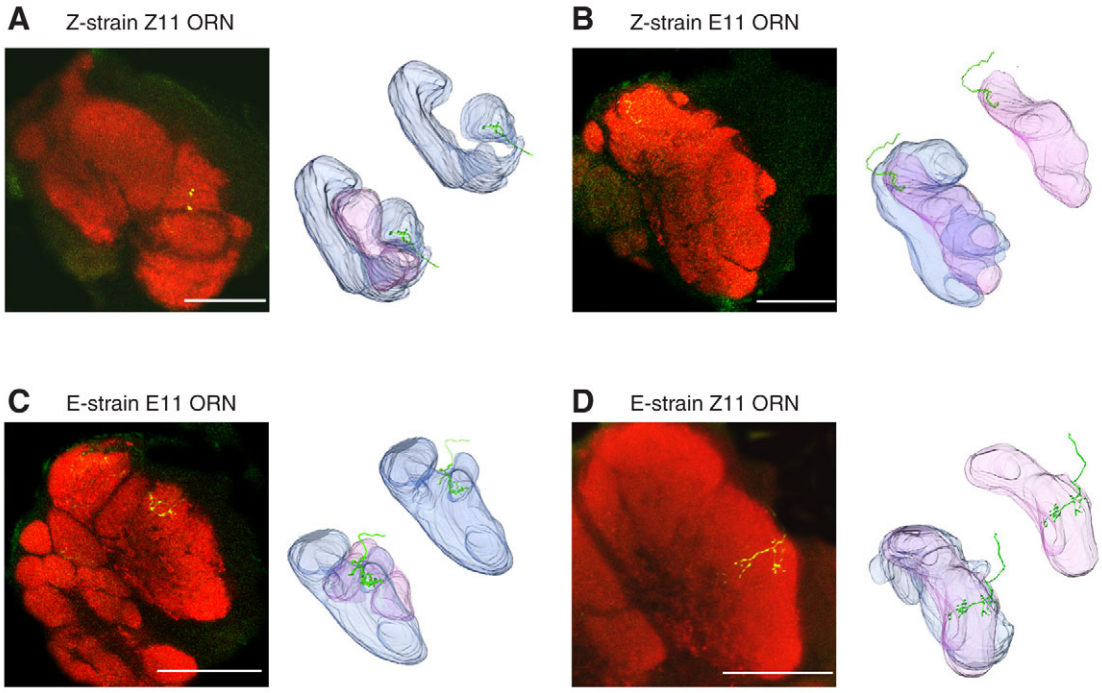

Fig. 2. Axonal projections into the macroglomerular complex (MGC) of olfactory receptor neurons (ORNs) after activity-dependent neurobiotin staining. ORN (yellow) in a red α-synapsin-labeled background. Left panel: confocal micrographs displaying part of the neuron. Note that to visualize large parts of the neuron several confocal sections were overlayed, which blurs glomerular delineations. Right panel: three-dimensional reconstruction of the two large MGC glomeruli (lateral, pink; medial, blue) and axonal projection of the ORN (green). For clarity, the glomerulus receiving axonal input is also shown excised from the MGC. (A) Anterograde staining of Z-male Z11-14:OAc-specific ORN. ORN axonal branches arborize in the medial glomerulus. (B) Anterograde staining of Z-male E11-14:OAc-specific ORN. Axonal arbors were found exclusively in the lateral MGC glomerulus. (C) Anterograde staining of E-male E11-14:OAc-specific ORN. Synapses are exclusively limited to the medial MGC glomerulus. (D) Anterograde staining of E-male Z11-14:OAc-specific ORN. Here the axon exclusively arborizes in the lateral MGC compartment. Scale bars, 50 μm.

Table 1. Number of recordings and stainings from projection neurons and olfactory receptor neurons in *O. nubilalis* males

		Projection neurons					ORNs		
Strain		E11	Z11	Z9	Blend	Total	E11	Z11	Total
E-strain	No. contacts					1278			180
	No. stains	20	33	2	5		17	48	
	No. successful stains	3	2	1	1		5	4	
Z-strain	No. contacts					538			125
	No. stains	15	25	–	8		12	9	
	No. successful stains	3	4	1	3		8	2	

Frequently more than one projection neuron (PN) was stained with neurobiotin due to multiple contacts. In addition, some attempts failed, whereas other stainings where incomplete. Therefore the rate of 'successful' stainings, i.e. a single complete PN stain, was rather low. Similarly activity-dependent staining from the antennae had a low success rate (14%). In cases where more than one ORN was stained, these invariably arborized each in a single macroglomerular complex glomerulus. Z11, Z11-14:OAc; E11, E11-14:OAc.

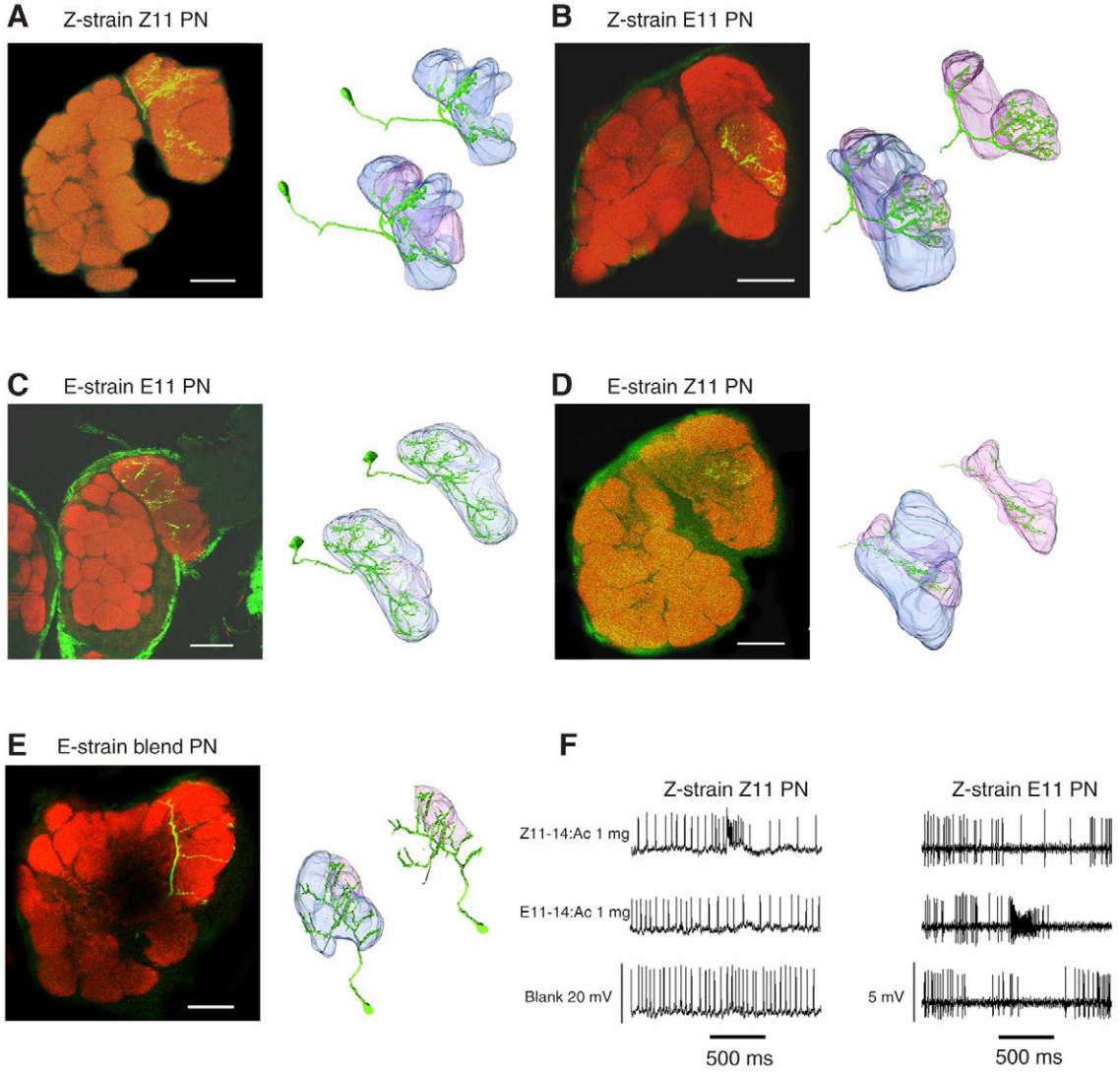

Fig. 3. Dendritic arborization patterns of projection neurons (PNs) in the macroglomerular complex (MGC) of *O. nubilalis*. PN (green) in a red α-synapsin-labeled background. Left panel: some confocal sections with part of the neuron visible. Note that to visualize large parts of the neuron several confocal sections were overlayed, which blurs glomerular delineations. Right panel: three-dimensional reconstruction of the two large MGC glomeruli (lateral, pink; medial, blue) and axonal projection of the olfactory receptor neuron (ORN; green). For clarity, the glomerulus receiving axonal input is also shown excised from the MGC. (A) The MGC of a Z-strain male displaying a Z11-14:OAc-specific PN staining with exclusive arborizations in the medial glomerulus. (B) The MGC of a Z-strain male displaying dendrites of E11-14:OAc-specific PNs only arborizing in the lateral glomerulus. (C) The MGC of an E-strain male displaying an E11-14:OAc-specific PN staining. E11-14:OAc-specific PNs arborized exclusively in the larger, medial MGC compartment. (D) As in C but now displaying a Z11-14:OAc-specific PN staining. In the E-strain, Z11-14:OAc-specific PN arborizations were restricted to the lateral MGC compartment. (E) A blend-specific PN, responding more strongly to a blend of Z11- or E11-14:OAc than the sum of the responses to the components separately, typically arborized in both large MGC glomeruli. (F) Typical responses of Z11- and E11-14:OAc-specific PN in the Z-strain. Scale bars, 50 μm.

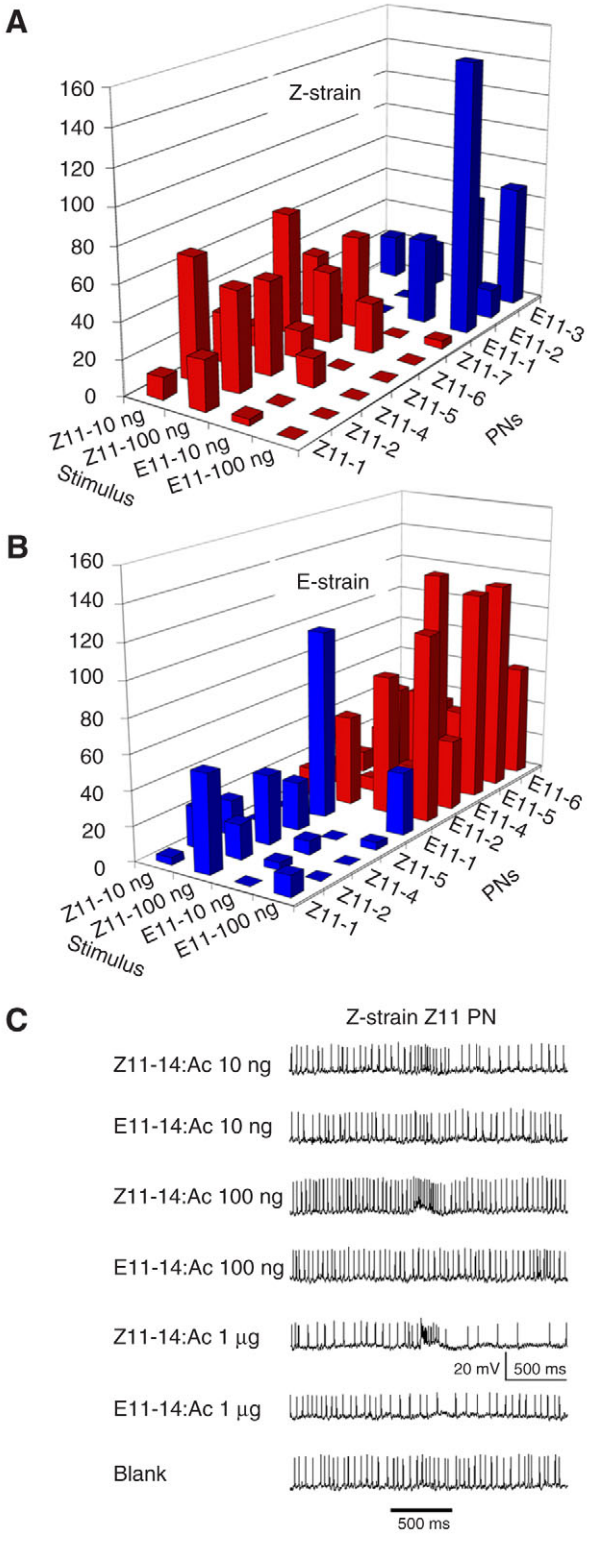

Fig. 4. Histograms of the response of specific PNs to E11- or Z11-14:OAc. Only preparations resulting in single PN stains are included. Empty squares indicate concentrations not tested on a specific neuron. In red are specific PNs that respond to the major pheromone component and in blue those that respond to the minor pheromone component. (A) Histogram of responses of Z-strain males to Z11- and E11-14:OAc (blue, E11-14:OAc PN; red, Z11-14:OAc PN). (B) Histogram of responses of E-strain males to Z11- and E11-14:OAc (blue, Z11-14:OAc PN; red, E11-14:OAc PN). (C) Sample dose–response trace of a Z-strain Z11-14:OAc-specific PN to Z11- and E11-14:OAc.

medial glomerulus and Z11-14:OAc-responding PNs arborizing into the lateral glomerulus (Fig. 3C,D). Both ORNs and PNs thus display innervation patterns opposite to those of the Z-strain. The two strains clearly have an identical MGC morphology, but a reversed functional topology. Table 2 summarizes the neuroanatomy and physiology of both strains of *O. nubilalis*.

DISCUSSION

Here we report on the neuroanatomy and neurophysiology of the AL of *O. nubilalis*. We were, for the first time, able to resolve the highly complex, intertwined MGC glomerular structures and to functionally classify the glomeruli this complex consists of.

Neuroanatomy and physiology of the macroglomerular complex

The neuroanatomy of the MGC of both Z- and E-strain *O. nubilalis* is indistinguishable. However, our extensive physiological analyses of the MGC in- and output, revealed a reversed physiological specificity. In both strains ORNs responding to the major pheromone component arborized in the large, medial MGC glomerulus, whereas the minor pheromone component-specific ORNs arborized in the smaller, lateral one. A similar morphology but changed physiology was also reported for heliothine species. The MGC of *Heliothis virescens* and *H. subflexa* was indistinguishable, but the physiology has in part changed to accommodate for the shift in pheromone blend preference (Vickers and Christensen, 2003).

We thus found a reversed functional topology in the MGC between the Z- and E-strain of the European corn borer. To account for the pheromone component representation in the two major MGC glomeruli, a similar change in the specificity and/or wiring of the sensory input must also have occurred. A possible explanation for our observations is a swap of olfactory receptors between ORNs within the same sensillum, while the ORN and PN arborization patterns in the MGC remain unaffected. Unlike the situation in mammals, insect ORs do not directly determine axonal targeting in the deutocerebrum (Dobritsa et al., 2003; Goldman et al., 2005; Endo et al., 2007; Ray et al., 2007). Previous genetic studies on the European corn borer revealed that a single, sex-chromosome linked factor is responsible for the reversed behavioral preference of the males for the two pheromone blends (Löfstedt et al., 1989; Dopman et al., 2004). In addition, an autosomal factor underlies a reversed action potential amplitude of Z11- and E11-14:OAc-responding ORNs between the Z- and E-strain (Hansson et al., 1987; Roelofs et al., 1987). Hybrids of Z- and E-strain *O. nubilalis* prefer an intermediate blend and show intermediate action potential amplitudes for both pheromone-responding cells. Yet, it is not clear how an OR swap would fit with the observation that the behavioral response is sex-linked, but the spike amplitude autosomal. Other possibilities include, for instance, that, instead of a single gene, a group of tightly-linked genes underlies the reversed antennal lobe physiology in *O. nubilalis*, which would allow for mechanisms such as rewiring of both ORNs to opposite MGC glomeruli. The matter is further complicated by the fact that Z11- and E11-14:OAc-sensitive ORNs are also found in other, much less frequent physiological subtypes of trichoid sensilla (Hallberg et al., 1994). *O. nubilalis* apparently expresses the same putative Z11- and E11-14:OAc-sensitive ORs in ORNs derived from different progenitor cells, while axons converge into the same glomerulus. Further research is needed on the cascade of events that determine the OR gene ‘choice’ of ORNs, and ORN axonal targeting to elucidate the mechanisms underlying the reversed physiological specificity of MGC-innervating projection neurons in *O. nubilalis*.

Table 2. Overview of the neuroanatomy and physiology of E- and Z-strain *O. nubilalis*

Strain	Pheromone Z11:E11	Neuron specificity	Target ORN	Glomerulus PN	Glomerular size (±s.d.; $\times 10^3$ μm^3)	Ratio M:L:P
Z-strain	97:3	Z11-14:OAc	M	M	297±36	
		E11-14:OAc	L	L	131±17	56:27:17
		Z9-14:OAc		P	89±3	
E-strain	1:99	Z11-14:OAc	L	L	111±26	
		E11-14:OAc	M	M	317±36	62:22:16
		Z9-14:OAc		P	81±17	

Z11, Z11-14:OAc; E11, E11-14:OAc; ORN, olfactory receptor neuron; PN, projection neuron; M, medial macroglomerular complex (MGC) glomerulus; L, lateral MGC glomerulus; P, posterior MGC glomerulus.

Macroglomerular complex blend neurons

Previous studies show that *O. nubilalis* has blend-specific AL neurons that are postulated to be crucial for the discrimination between blends (Anton et al., 1997). We also found PNs that displayed a stronger response to a blend of Z11 and E11 than the added responses to the components separately (Fig. 3E). The cell bodies of these PNs were located in the lateral cell cluster, which matches similar findings in *B. mori* (Kanzaki et al., 2003), *A. segetum* (Hansson et al., 1994a), *H. zea* and *H. virescens* (Christensen et al., 1989; Christensen et al., 1991) blend-specific PNs. It remains to be seen whether there is indeed a strict correlation between PN neuroanatomy, physiology and soma position. Of particular interest is whether such neurons are essential to the readout of the ratio of pheromone components and of behavioral importance. In *Drosophila*, such a relationship does not hold (Marin et al., 2002; Wong et al., 2002). How these differences may be relevant to olfactory behavior is thus still unclear.

Large female glomeruli (LFG)

Female *O. nubilalis* also possess enlarged glomeruli at the entrance of the antennal lobe, which are homologues to those found in other species and have been called large female glomeruli (LFG) in *M. sexta* (Roche King et al., 2000; Rossler et al., 1998). In females *Heliothis virescens* the ORNs tuned to one of the sex pheromone components arborize in the female-specific central large female glomerulus (cLFG) and other glomeruli in the AL (Hillier et al., 2006). By contrast, the LFGs of *M. sexta* seem to receive innervation from ORNs tuned to host odor volatiles. In electroantennogram (EAG) studies, antennae of females *O. nubilalis* Z-strain respond to Z11-14:OAc (Z.K., unpublished observations). In further studies we will study the physiology of the female AL, including the two LFGs.

Numerical invariance in total number of glomeruli in Lepidoptera

Our reconstruction of the ALs of *O. nubilalis* further shows that the total number of glomeruli (♀ ~64 and ♂ ~66) closely approximates that found in other Lepidoptera: *Mamestra brassicae* – 67 ♂, 68 ♀ (Rospars, 1983), *Manduca sexta* – 63 (Rospars and Hildebrand, 2000), *Heliothis virescens* – 66 ♂, 62 ♀ (Berg et al., 2002), *Bombyx mor* – ~60 (Kanzaki et al., 2003), *Agrotis ipsilon* – 66 (Greiner et al., 2004), which implies relative constancy in the number of different ORN types and the number of ORs expressed. The high numerical invariance of moth AL glomeruli, around ~64, in distantly related moth taxa is striking, especially considering the large niche diversification in Lepidoptera. By contrast, Hymenoptera species show a high variance in number of glomeruli even between closely related species or within castes of the same species [e.g. *Apis mellifera* worker: 166 glomeruli, drone: 103 glomeruli (Arnold et al., 1985); *Vespa crabro* ~1000 glomeruli (Hanström, 1928)]. The invariance in the number of glomeruli raises the question of how the olfactory circuitry could accommodate the enormous niche differentiation observed in Lepidoptera. An alternative route for evolution of olfactory preference is evolution of the ORs themselves. Minor changes in amino acid sequences may affect the binding affinity (e.g. Dekker et al., 2006), although strikingly high conservation of physiological response characteristics of ORNs has been reported too (Stensmyr et al., 2003; Ray et al., 2007; McBride, 2007).

We thank Wen-Qi Wu for initial assistance with electrophysiology, and Sylvia Anton, Mikael Carlsson, Wiltrud Daniels, Medhat Sadek, Wendell Roelofs, Gábor Szöcs. We also would like to thank the two anonymous reviewers for their helpful suggestions. This project was supported by grants from the Swedish Research Council (VR) to B.S.H. and from Formas to T.D. It was also strongly supported by the Linnaeus Grant 'Insect Chemical Ecology, Ethology and Evolution (ICE^3)' and the Hungarian National Science Foundation (OTKA: K 71980).

REFERENCES

Anglade, P., Stockel, P. and Cooperators, I. (1984). Intraspecific sex-pheromone variability in the European corn borer, *Ostrinia nubilalis* Hbn. (Lepidoptera, Pyralidae). *Agron. J.* **4**, 183-187.

Anton, S. and Hansson, B. S. (1994). Central processing of sex pheromone, host odour and oviposition deterrent information by interneurones in the antennal lobe of female Spodoptera littoralis (Lepidoptera: Noctuidae). *J. Comp. Neurol.* **350**, 199-214.

Anton, S. and Hansson, B. S. (1995). Sex pheromone and plant-associated odour processing in antennal lobe interneurones of male *Spodoptera littoralis* (Lepidoptera: Noctuidae). *J. Comp. Physiol. A* **176**, 733-789.

Anton, S., Löfstedt, C. and Hansson, B. S. (1997). Central nervous processing of sex pheromone in two strains of the European corn borer *Ostrinia nubilalis* (Lepidoptera: Pyralidae). *J. Exp. Biol.* **200**, 1073-1087.

Arnold, G., Masson, C. and Budharugsa, S. (1985). Comparative study of the antennal lobes and their afferent pathway in the workbee and the drone *Apis mellifera* L. *Cell Tissue Res.* **242**, 593-605.

Berg, B. G., Almaas, T. J., Bjaalie, J. G. and Mustaparta, H. (1998). The macroglomerular complex of the antennal lobe in the tobacco budworm moth *Heliothis virescens*: specified subdivision in four compartments according to information about biologically significant compounds. *J. Comp. Physiol. A* **183**, 669-682.

Berg, B. G., Galizia, C. G., Brandt, R. and Mustaparta, H. (2002). Digital atlases of the antennal lobe in two species of tobacco budworm moths, the oriental *Helicoverpa assulta* (male) and the American *Heliothis virescens* (male and female). *J. Comp. Neurol.* **446**, 123-134.

Bretschneider, F. (1924). Über die Gehirne des eichenspinners und des Seidenspinners (*Lasiocampa quercus* L. und *Bombyx mori* L.). *Jena. Z. Naturw.* **60**, 563-570.

Cardé, R. T., Roelofs, W. L., Harrison, R. G., Vawter, A. T., Brussard, P. F., Mutuura, A. and Munroe, E. (1978). European corn borer: Pheromone polymorphism or sibling species? *Science* **199**, 555-556.

Christensen, T. A. and Hildebrand, J. G. (1987). Male-specific sex pheromone-selective projection neurons in the antennal lobes of the moth *Manduca sexta*. *J. Comp. Physiol. A* **160**, 553-569.

Christensen, T. A., Mustaparta, H. and Hildebrand, J. G. (1989). Discrimination of sex pheromone blends in the olfactory system of the moth. *Chem. Senses* **14**, 463-477.

Christensen, T. A., Mustaparta, H. and Hildebrand, J. G. (1991). Chemical communication in heliothine moths. II. Central processing of intraspecific and interspecific olfactory messages in the male corn earworm moth, *Helicoverpa zea*. *J. Comp. Physiol. A* **173**, 385-399.

Cossé, A. A., Campbell, M. G., Glover, T. J., Linn, C. E., Todd, J. L., Baker, T. C. and Roelofs, W. L. (1995). Pheromone behavioral responses in unusual male

European corn borer hybrid progeny not correlated to electrophysiological phenotypes of their pheromone-specific antennal neurons. *Experientia* **51**, 809-816.

Dekker, T., Ibba, I., Siju, K. P., Stensmyr, M. C. and Hansson, B. S. (2006). Olfactory shifts parallel superspecialism for toxic fruit in *Drosophila melanogaster* sibling, *D. sechellia*. *Curr. Biol.* **16**, 101-109.

Dobritsa, A. A., van der Goes van Naters, W., Warr, C. G., Steinbrecht, A. and Carlson, J. R. (2003). Integrating the molecular and cellular basis of odor coding in the *Drosophila* antenna. *Neuron* **37**, 827-841.

Endo, K., Aoki, T., Yoda, Y., Kimura, K. and Hama, C. (2007). Notch signal organizes the *Drosophila* olfactory circuitry by diversifying the sensory neuronal lineages. *Nat. Neurosci.* **10**, 153-160.

Glover, T. J., Perez, N. and Roelofs, W. L. (1989). Comparative analysis of sex-pheromone-responses antagonists in three races of European corn borer. *J. Chem. Ecol.* **15**, 863-873.

Goldman, A. L., van der Goes van Naters, W., Lessing, D., Warr, C. G. and Carlson, J. R. (2005). Coexpression of two functional odor receptors in one neuron. *Neuron* **45**, 661-666.

Greiner, B., Gadenne, C. and Anton, S. (2004). Three-dimensional antennal lobe atlas of the male moth, *Agrotis ipsilon*: A tool to study structure-function correlation. *J. Comp. Neurol.* **475**, 202-210.

Hallberg, E., Hansson, B. S. and Steinbrecht, R. A. (1994). Morphological-characteristics of antennal sensilla in the European corn borer *Ostrinia nubilalis* (Lepidoptera, Pyralidae) *Tissue Cell* **26**, 489-502.

Hansson, B. S. (1997). Antennal lobe projection patterns of pheromone-specific olfactory receptor neurons in moths. In *Insect Pheromone Research: New Directions* (ed. R. T. Carde and A. K. Minks), pp. 164-183. New York: Chapman & Hall.

Hansson, B. S., Löfstedt, C. and Roelofs, W. L. (1987). Inheritance of olfactory response to sex pheromone components in *Ostrinia nubilalis*. *Naturwissenschaften* **74**, 497-499.

Hansson, B. S., Ljunberg, H., Hallberg, E. and Löfstedt, C. (1992). Functional specialization of olfactory glomeruli in a moth. *Science* **256**, 1313-1315.

Hansson, B. S., Anton, S. and Christensen, T. A. (1994a). Structure and function of antennal lobe neurons in the male turnip moth, *Agrotis segetum* (Lepidoptera: Noctuidae). *J. Comp. Physiol. A* **175**, 547-562.

Hansson, B. S., Hallberg, E., Löfstedt, C. and Steinbrecht, R. A. (1994b). Correlation between dendrite diameter and action potential amplitude in sex pheromone specific receptor neurons in male *Ostrinia nubilalis* (Lepidoptera: Pyralidae). *Tissue Cell* **26**, 503-512.

Hanström, B. (1928). Vergleichende Anatomie des Nervensystems der wirbellosen Tiere. Berlin: Springer.

Hillier, N. K., Kleineidam, C. and Vickers, N. J. (2006). Physiology and glomerular projections of olfactory receptor neurons on the antenna of female *Heliothis virescens* (Lepidoptera: Noctuidae) responsive to behaviorally relevant odors. *J. Comp. Physiol. A* **192**, 199-219.

Kanzaki, R., Soo, K., Seki, Y. and Wada, S. (2003). Projections to higher olfactory centers from subdivisions of the antennal lobe macroglomerular complex of the male silkmoth. *Chem. Senses* **28**, 113-130.

Kirschner, S., Kleineidam, C. J., Zube, C., Rybak, J., Grünewald, B. and Rössler, W. (2006). Dual olfactory pathway in the honeybee, *Apis mellifera*. *J. Comp. Neurol.* **499**, 933-952.

Klun, J. A. and Robinson, J. F. (1971). European corn borer moth: Sex attractant and sex attraction inhibitors. *Ann. Entomol. Soc. Am.* **64**, 1083-1086.

Klun, J. A., Chapman, O., Mattes, J. C., Wojtkowski, P. W., Beroza, M. and Sonnett, P. E. (1973). Insect sex pheromones: minor amount of opposite geometrical isomer critical to attraction. *Science* **181**, 661-663.

Koontz, M. A. and Schneider, D. (1987). Sexual dimorphism in neuronal projections from the antennae of silk moths (*Bombyx mori*, *Antherea polyphemus*) and the gypsy moth (*Lymantria dispar*). *Cell Tissue Res.* **249**, 39-50.

Löfstedt, C., Hansson, B. S., Roelofs, W. L. and Bengtsson, B. O. (1989). No linkage between genes controlling female pheromone production and male pheromone response in the European corn borer, *Ostrinia nubilalis* Hübner (Lepidoptera; Pyralidae). *Genetics* **123**, 553-556.

Malausa, T., Bethenod, M.-T., Bontemps, A., Bourguet, D., Cornuet, J.-M. and Ponsard, S. (2005). Assortative mating in sympatric host races of the European corn borer. *Science* **308**, 258-260.

Mani, E., Riggenbach, W. and Mendik, M. (1978). Zucht des Apfelwicklers (*Lasperyesia pomonella* L.) auf künstlichem Nährboden, 1968-1978. *Mitt. Schweiz. Entomol. Ges.* **51**, 315-326.

Marin, E. C., Jefferis, G. S. X. E., Komiyama, T., Zhu, H. and Luo, L. (2002). Representation of the glomerular olfactory map in the *Drosophila* brain *Cell* **109**, 243-255.

McBride, C. S. (2007). Rapid evolution of smell and taste receptor genes during host specialization in *Drosophila sechellia*. *Proc. Natl. Acad. Sci. USA* **104**, 4996-5001.

Ochieng, S. A., Anderson, P. and Hansson, B. S. (1995). Antennal lobe projection patterns of olfactory receptor neurons involved in sex pheromone detection in *Spodoptera littoralis* (Lepidoptera: Noctuidae). *Tissue Cell* **27**, 221-232.

Ray, A., van der Goes van Naters, W., Shiraiwa, T. and Carlson, J. R. (2007). Mechanisms of odor receptor gene choice in *Drosophila*. *Neuron* **53**, 353-369.

Roche King, J., Christensen, T. A. and Hildebrand, J. G. (2000). Response characteristics of an identified, sexually dimorphic olfactory glomerulus *J. Neurosci.* **20**, 2391-2399.

Roelofs, W. L. and Glover, T. J. (1991). Genetics of a moth pheromone system. In *Chemical Senses*, vol. 3 (ed. C. J. Wysocki and M. R. Kare), pp. 109. New York: Marcel Decker.

Roelofs, W. L., Glover, T. J., Tang, X.-H., Robbins, P. S., Löfstedt, C., Hansson, B. S., Bengtsson, B. O., Sreng, I. and Eckenrode, C. J. (1987). Sex pheromone production and perception in European corn borer moths is determined by both autosomal and sex-linked genes. *Proc. Natl. Acad. Sci. USA* **84**, 7585-7589.

Rospars, J. P. (1983). Invariance and sex-specific variations of the glomerular organization in the antennal lobes of a moth, *Mamestra brassicae*, and a butterfly, *Pieris brassicae*. *J. Comp. Neurol.* **220**, 80-96.

Rospars, J. P. and Hildebrand, J. G. (2000). Sexually dimorphic and isomorphic glomeruli in the antennal lobes of the sphinx moth *Manduca sexta*. *Chem. senses* **25**, 119-129.

Rossler, W., Tolbert, L. P. and Hildebrand, J. G. (1998). Early formation of sexually dimorphic glomeruli in the developing olfactory lobe of the brain of the moth *Manduca sexta*. *J. Comp. Neurol.* **396**, 415-428.

Stensmyr, M. C., Giordano, E., Balloi, A., Angioy, A. M. and Hansson, B. S. (2003). Novel natural ligands for *Drosophila* olfactory receptor neurons. *J. Exp. Biol.* **206**, 715-724.

Todd, J. L., Anton, S., Hansson, B. S. and Baker, T. C. (1995). Functional organization of the macroglomerular complex related to behaviorally expressed olfactory redundancy in male cabbage looper moth. *Physiol. Entomol.* **20**, 349-361.

Vickers, N. J. and Christensen, T. A. (2003). Functional divergence of spatially conserved olfactory glomeruli in two related moth species. *Chem. Senses* **28**, 325-338.

Wong, A. M., Wang, J. W. and Axel, R. (2002). Spatial representation of the glomerular map in the *Drosophila* protocerebrum *Cell* **109**, 229-241.

Wu, W.-Q., Anton, S., Löfstedt, C. and Hansson, B. S. (1996). Discrimination among pheromone component blends by interneurons in male antennal lobes of two populations of the turnip moth, *Agrotis segetum*. *Proc. Natl. Acad. Sci. USA* **93**, 8022-8027.